ISSN 2229-5518

Influence of annealing on structural and Micro- Hardness of nanocrystalline TiO_2 Thin Films

F. Abd El-Salam, M. M. Mostafa, M.M. El-Nahass, R.H.Nada, E.F. M. El Zaidia, H.S. Mohamed*

Physics Department, Faculty of Education, Ain Shams University, Roxy 11757, Cairo, Egypt

Abstract: In the present study, TiO_2 powder was used as the starting material to prepare thin films by conventional thermal evaporation using high vacuum coating unit type (Edwards E 306A). The surface topography and nanoparticles shape of TiO_2 thin films as deposited and annealed at the temperatures 473, 673 and 873K were studied using the scanning electron microscope. The films showed good uniformity, crack free surface and nanoparticles with small ellipsoidal shape dispersing with high separations. The indentation experiments were carried out by using micro hardness tester showed the absence of monotonic behaviour and irregular thermally induced oscillations in the curves of the film hardness, HVf versus the annealing temperature. This behavior may be due to the combined effects of the applied factors; the temperature, the load and the dwell time, on the obtained HVf. Also the indentation size effect index (ISE), m, was calculated as 1.6 for the TiO_2 films indicating that the hardnesss depends on indentation size.

Keywords: TiO_2; Annealing thin films; Nanoparticles; Vickers Hardness; Indentation Size Effect.

————————— ◆ —————————

IJSER

1- Introduction:

Nanocrystalline materials show interesting properties due to their large active surface to volume ratio [1]. Titanium dioxide (TiO_2) which belongs to the family of nanoparticle transition metal oxides has more attention nowadays due to its unique mechanical, electrical, chemical and optical properties. It should be noted that, the particle-size of TiO_2 plays a dominant role in determining its physical properties.

Titanium dioxide (TiO_2) exists in three major polymorphs crystals: anatase (tetragonal, a=0.3782nm, c=0.9502nm), rutile (tetragonal, a=0.4584nm, c=0.2953nm) and brookite (orthorhombic a= 0.5436nm, b= 0.9166nm, c= 0.5135nm) [2]. TiO_2 has received a great attention due to its non-toxicity [3], wide band gap, interesting chemical, electrical and optical properties, and high thermal and good chemical stability in various environments. [4]. TiO_2 has also applications at antifogging mirror and glass, and the American Food and Drug Administration (FDA) has approved the use of TiO_2 in human food, drugs, and materials in contact with unprotected food [5-8]. Anatase TiO_2 phase is a more photoactive material because of its higher electron mobility, low dielectric constants and lower density, lower deposition temperature and chemically active [9, 10].

In batteries, the anatase form is used as an anode material in which lithium ions can intercalate reversibly [11].

The obtained structure and mechanical properties of TiO_2 thin films depend on the preparation method and the deposition conditions [12]. TiO_2 nanostructure thin films are prepared by various methods including the thermal evaporation method [13], which is adopted in the present work. Study of the mechanical properties of TiO_2 thin films is practically important in the application of optical coatings.

The presenet work aims to study the effect of heat treatment on the surface topography and the hardness variations of TiO_2 nanoparticles thin films grown by the conventional thermal evaporation. This is attained by analysing the hardness data due to a mathematical model to avoid the effect of substrate on the film properties.

2. Experimental technique:

Titanium dioxide (TiO_2) supplied by Millennium inorganic chemicals, SP-300N A Cristal Company, France, was used in a colloidal suspensions of nanocrystalline TiO_2 particles as the starting material. These colloidal suspensions of nanocrystalline TiO_2 particles were painted onto glass substrates then dried in air at room temperature for several hours, until white crystals appeared. These crystals were crushed and ground to fine powder. TiO_2 thin films were prepared by the conventional thermal evaporation technique, using the TiO_2 powder form as a target in a high vacuum coating unit type (Edwards E 306A) to be evaporated as nanostructure thin films onto pre-cleaned soda lime glass substrates. The substrates were mounted on rotatable holder of (30 rps) at 25 cm from an evaporator, crucible boat, charged with a suitable amount of TiO_2 powder to allow homogenous distribution of the film thickness. When the vacuum chamber was pumped down to vacuum level of (2×10^{-4} Pa), it was assisted by liquid nitrogen during the thermal evaporation process. The boat was heated by a tungsten coil and the heating current was increased gradually until the evaporation process started. The coating unit is supplied by a quartz crystal monitor (FTM4, Edwards), to control the deposition rate and simultaneously to measure the thickness of the deposited film. The constant deposition rate 2 nm /s was kept until the required thickness was obtained.

The film thickness measured by the monitor was checked by Tolansky's interferometric method [14]. Three different thicknesses of TiO_2 films, 164, 229, and 263nm, were prepared. The deposited film with the thickness 263nm as example was annealed at 473, 673, and 873K using an electric furnace for 4 hours. X-ray diffraction patterns of TiO_2 in the powder and thin film forms were recorded on a Philips X-ray diffractometer (model X' Pert) using Ni-filtered, Cuk_α radiation (λ=1.5418 Å), a voltage of 40 kV, and 25 mA current.

The surface topography for TiO_2 thin films was investigated by the scanning electron microscopy (SEM) model JEOL5410(Japan) with accelerating voltage 30 KV, magnification 15X up to 200,000X (25 steps) and resolution 3.5 nm (at 30 kV).

It is well-known that hardness indentation tests have been widely used to characterize the mechanical properties of various materials at the micro/nanometer scales such as metals, diamond-like carbon, polymers, ceramics etc. [15-17].

the hardness depends on the indentation depth or load, exhibiting the well-known Indentation Size Effect (ISE). Therefore, the effect of grain size, solution or precipitation strengthening and strain hardening are particularly relevant. Refining the grain size, d of a polycrystalline metal increases the tensile flow stress that is commonly quantified by the empirical Hall-Petch relation [18].

So, in order to determine the mechanical properties of nanostructured TiO_2 thin films, hardness test was carried out using a hardness tester (Model (HWDM7, TSS – Japan) fitted with a Vickers diamond pyramidal indenter. The measurements were performed on the film surface of the film/substrate system. The thin film systems were indented at different sites for the deposited film with thickness 164, 229, and 263nm, and the film of thickness 263nm annealed for 4 h. at 473,673, and 873K with applying automatically the loads (10, 50, 100, 300 gm) for the dwell times (10, 20, 30,40 and 50 sec). Each hardness data point represents the average of each 3 to 5 data points. The effects caused by elastic recovery, pile-up and curvature of the indenter tip were neglected. The two lines, which move to opposite sides to identify the indentation diagonals, were adjusted to these edges and the end button on the tester

IJSER

was pressed to show the mean diagonal value, d, and the corresponding hardness value, H_v. All measurements have been performed in air at room temperature. Direct determination of true film hardness of the thin films is not possible when the indentation depth is more than 10% is the film thickness. In order to determine the true film hardness H_{Vf} in our studies, we used a model based on the energy expended during indentation. Their assumption is that the work of deformation can be broken into plastic deformation of the substrate and the deformation and fracture of the coating it was proposed by A. M. Korsunsky et al [19], for the Vickers indentation, which analyzed the measured hardness data using dimensionless parameters considered either plasticity- or fracture-dominated behavior ,using the equation:

$$H_{VC} = H_{Vs} + \frac{H_{Vf} - H_{Vs}}{1 + k\beta^2} \quad (1)$$

where H_{VC} is the composite measured hardness which measured for film/substrate system, H_{VS} is the hardeness of substrate, H_{Vf} is the film hardness, β denotes the indentation depth D normalized with respect to the coating thickness t and has been termed the relative indentation depth,RID, i.e $\beta=D/t$, and $k=t/\alpha$ where the parameter α having the dimension of length, depend on the ratio G_C/H_{VS} (G_C denotes the through- thickness fracture toughness of the coating) for fracture-dominated case and α be largely proportional to the coating thickness t, for plasticity- dominated case. The model can describes very well the behavior of the coated system over a large range of indentation scales but fails to predict the hardness of the film when there is no sufficient data in the micro-indentation range. The film hardness can be determined by the experimentally determined variation of H_{VC} with β. The data of the composite hardness measured at 10, 50, 100, 300 g with different dwell time, so the parameters H_{VS}, H_{Vf} , k determined by fitting the relation between H_{VC} and β using equation (1).

IJSER

3. Results and discussion:

3.1. X-ray diffraction studies of TiO_2 in powder and thin film forms

XRD patterns of TiO_2 in powder form, the as deposited film and the annealed films for 4 h. at the temperatures (673,873 and 1073K) are shown in Fig.1.

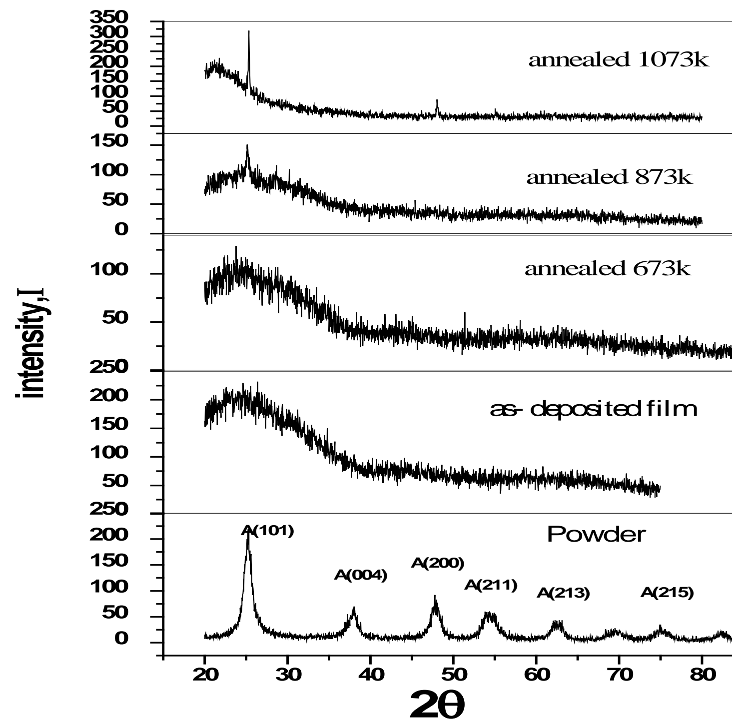

Fig.1 XRD patterns of TiO_2 in powder form, the as deposited film and the annealed films for 4 h. at the temperatures (673,873 and 1073K).

The powder XRD pattern In Fig.1, shows many peaks with different intensities indicating that the material is composed of irregular polycrystallines. The Miller indices (hkl) given on each diffraction peak, which are due to the standard spectrum (JCPDS Card84-1286), show good agreement with a tetragonal structure crystal for TiO_2 anatase phase with lattice parameters a=b=3.7822 Å and c=9.46596 Å. The particle size, D, can be calculated according to the Scherrer formula [20]:

$$D = \frac{K_s \lambda}{\beta \cos\theta}, \qquad (2)$$

where λ is the X-ray wavelength, θ is the corresponding Bragg angle , K_s is the Scherrer's constant, which has the order unity (~ 0.9) and β is the full-width at half maximum, FWHM, of the Bragg peak in radians. From all the observed planes of the TiO_2 anatase phase the average particle size, D, obtained for the powder is 30.266nm.

X-ray diffraction XRD pattern for TiO_2 as–deposited thin film of thickness (263nm), given in Fig.1 shows that no diffraction peaks are observed indicating an amorphous broad pattern with low intensity, except a broad peak around $2\theta = 25^{\circ}$. However, the effect of amorphous materials on the broadening of the XRD patterns of nanosized TiO_2 is negligible. The effect of annealing on the structure of the amorphous as-deposited TiO_2 film is observed from the XRD shown in Fig.1 obtained after annealing the as–deposited films at 673,873 and 1073K for 4 h. The amorphous as–deposited films after annealing at 673K, showed a polycrystalline structure. For the TiO_2 thin film annealed at 873K, the observed plane (101) which shows that the

ISSN 2229-5518

strongest reflection, with intensity, I= 100%, showed good agreement with a tetragonal structure crystal for TiO_2 anatase phase, The particle size, D, according to the Scherrer formula was calculated as 33.5 nm. By increasing the annealing temperature to 1073K the particle size from (101) plane increased to 36.2 nm.

3.2. Topological properties of TiO_2 thin films:

The surface topography and grain shape growth of TiO_2 nanoparticles for as-deposited and annealed thin films were studied using the scanning electron microscopy, SEM, as shown in Fig. 2.

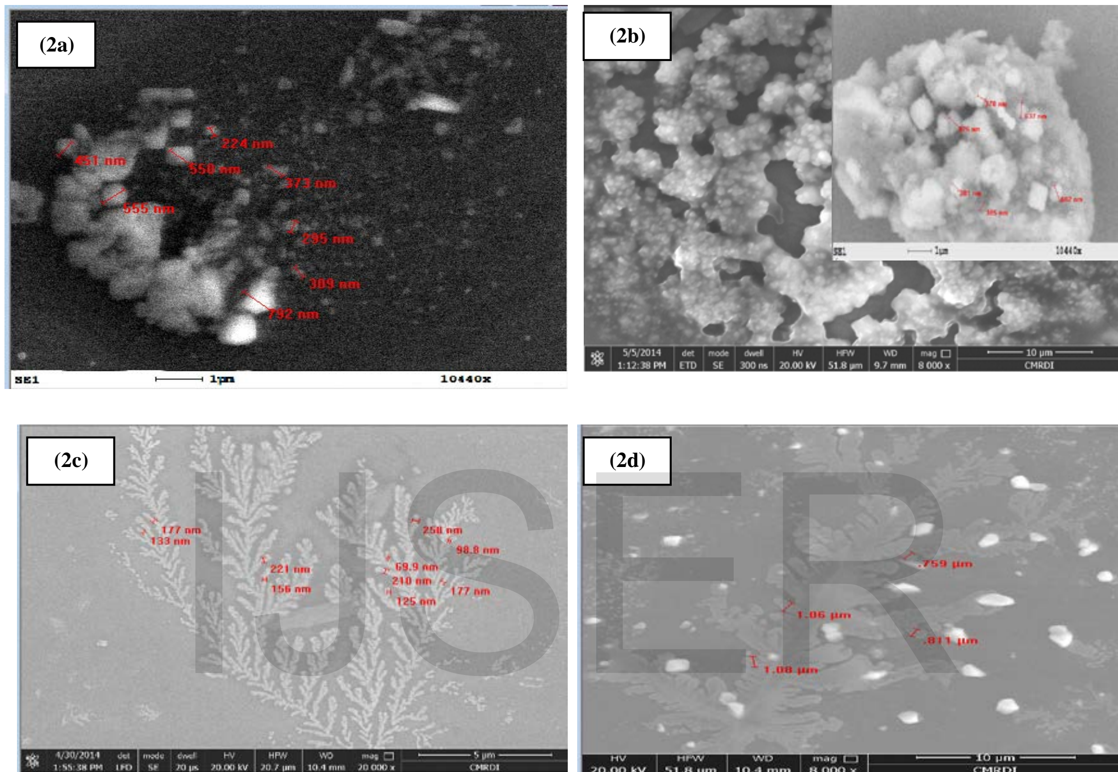

Fig.2 (a-d): SEM micrographs for as-deposited annealed for 4 h. at temperatures 473, 673 and 873K TiO_2 thin films.

Fig. (2-a) shows the SEM image of as-deposited thin film on glass substrate. TiO_2 nanoparticles dispersing with high separations are observed with small ellipsoidal shape in order of nano size.

The surface topography of the annealed TiO_2 films at 473K shown in Fig.2b, reflects the nature of amorphous phase of agglomerated separated large particles. These agglomerates are constituted by interconnected nanoparticles and reveals dendrite- like morphology by increasing the annealing temperature.

In Figs.2.c and 2.d the presence of deferent impurity elements can act as seed structures that allow the formation of dendritic structure appears to grow in a diffusion-limited aggregation (DLA) process [21].

At 673K, the film in Fig. 2 c, where the line thickness of the dendrites is nearly close to the diameter of the titania nanospheres, showing thinner and more clearly defined dendritic structures of leaves-shaped form with no slippage. These dendrite structures are formed according to the orientations of the lattice fringes indicating the established crystallinity of TiO_2 crystallites. So, the 673K might be an optimum temperature to achieve crystallization and

minimize the thermal growth of the crystallites at 673K maintaining the nanoscale features. Increasing annealing temperature to 873K, the average size of dendritic structures increased making the nature of the TiO_2 anatase film in Fig. 2- d as an improved state of that in Fig.2- c at 673K. This may be due to the change of TiO_2 anatase phase from amorphous to polycrystalline nature after annealing at about 673K, and due to the variations in the lattice parameters at this temperature, the film becomes under tensile strain [22]. The SEM result is in agreement with the particle size results obtained from XRD patterns that indicate an increase in nano-particles size on increasing annealing temperature.

3.3 Hardness measurements:

In this regard, hardness H as a rapid, inexpensive, none destructively in-situ becomes a handy tool for evaluating the integrity of metallic structures and measuring mechanical properties at elevated temperatures [23, 24].

The micro hardness, H_v, was calculated as; [25].

$$H_V = 1.8544\, p/(d)^2 \text{ Kg/mm}^2 \quad (3)$$

where p is the applied load in Kg, and d is the average diagonal length of the Vickers impression in mm after unloading.

Indentation micro hardness measurements have been increasingly used for mechanical characterization of surfaces and thin films [24, 25], such as physical vapour- deposited TiN [26]

The measured apparent hardness of thin film includes contributions of both the film and substrate when some critical indentation depth is surpassed.
Different mathematical models are developed to separate these contributions [27-32].

Appling Korsunsky [19], model (Eq.1) the contribution of both the film and the substrate was separated as follows.

The film hardness values can be determined through the experimental determined variation between H_{VC} and β. From the obtained composite hardness data measured under 10, 50, 100, 300 g at dwell time 10 sec., the parameters H_{VS}, H_{Vf} , k obtained by fitting the relation between H_{VC} and β using equation3, are shown in table1.

Table 1.4: Curve-fit data produced from the model (model used: $H_C=H_s+ (\Delta H/1+ k*\beta^2)$; input starting values for the fit H_s=274.0213; ΔH =115.5; k=-0.00813) [19].

Temperature of the Film (t, thickness, =0.263μm)	H_{VS} (Kg/mm^2)	ΔH (Kg/mm^2)	H_{Vf} (Kg/mm^2)	k
As deposited	220.39	227.59	447.97	-0.00438
473K	157.91	172.51	330.4	-0.00625
673K	335.3	331.098	666.398	0.00164
873K	334.052	334.052	668.104	1.916×10^{-5}

Also, the composite hardness measured data under 10, 50, 100, 300 g at different dwell times were analyzed by the same model.

Fig. 3 shows the hardness values, H_{Vf}, of the as-deposited TiO_2 films with the thickness values: 164, 229, and 263 nm, under the load, p=50g, and dwell time, t=20 sec. the film hardness values determined applying Korsunsky model [19] for all thicknesses.

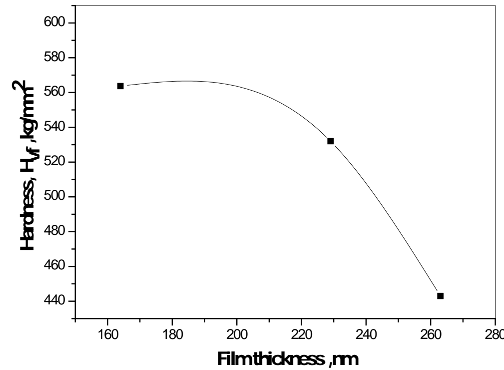

Fig.3: Variation of Vickers hardness, H_{Vf}, and thickness of as-deposited TiO_2 thin films.

Increasing film thickness, the hardness decreases due to the decrease in film density [33]. This agrees well with previous investigations [34, 35].

The temperature dependence of hardness, H_{Vf}, with dwell times 10, 20, 30, 40, and 50 sec, for TiO_2 films is given in Fig.4 .

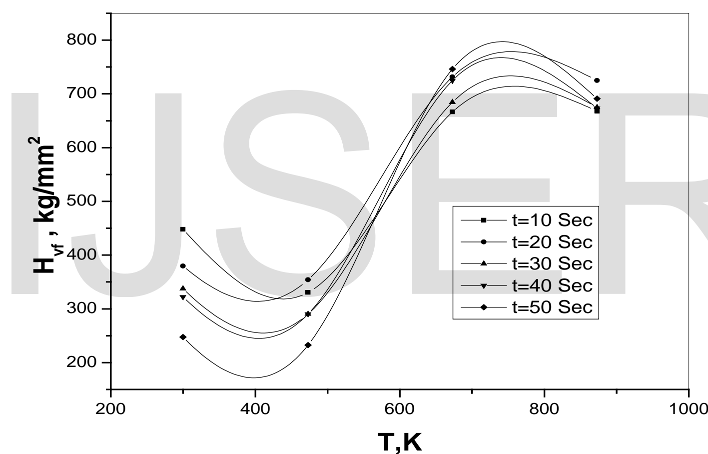

Fig.4 : Temperature dependence of hardness, H_{vf} at different dwell times.

The absence of stable monotonic behaviour, the irregular thermally induced oscillations and the wavy form of the, H_{Vf} - T, curves in Fig. 4, may be due to the combined effects of the applied factors T, and t, and the constant load, p. on H_{Vf}, which reflect mainly the instable nature of the internal structure existing at certain temperature. So, increasing temperature causes structural modifications, which are responsible for changes in hardness levels.

It was found [34] that the decrease of both the hardness and elastic modulus on annealing above 573K, where the crystalline structure was not observed, is due to the Na diffusion from the substrate which has a lack of the substrate bias on an insulating glass substrate [35].

In a systematic study [21], it was found that annealing above 573k, decreases both the hardness and the elastic modulus due to the thermal diffusion of Na ions from the glass substrate. Besides Na effect, the increase in particle size makes the temperature 573K an optimal annealing temperature where annealing above 573k is therefore, an effect related to the substrate [33].

The inceased strengthening in the film, which results due to a decrease in lattice constant is stronger than that due to an increase in lattice constant [36]. The lattice parameters (a, c) estimated for the tetragonal unit cell of TiO_2 anatase depend on annealing temperature where the lattice constant, a, decreased with increasing the annealing temperature while the lattice constant, c, increased. The value of the ratio c/a for the film annealed at 673K is lower than that for a stress free TiO_2 phase [37], so this film is under tensile strain showing crystallite size of 16 nm, while this ratio for the film annealed at 873K is close to that of the stress free TiO_2 showing crystallite size of 19 nm [38].

Thermal effect can be considered as important source for the observed irregular hardness changes. The relationship between hardness H and temperature (T) reported in [39], has the form;

$$H = H_0 \exp(-\alpha T) \quad (4)$$

where H_0 is the intrinsic hardness, or the hardness at zero K, and α is the softening coefficient, [14] or the coefficient of thermal expansion [40] .

It was reported that hardness decreases with indentation time, according to the form [41],

$$H = H_1 t^{-k} \quad (5)$$

where H_1 is the hardness at a given reference time t =1 and k is the so-called creep constant which has the relation, $k = -1/m$, where m is the stress exponent.

The samples in Fig. 4, annealed in air for 4 h, have quite different behaviour, than that for vacuum annealed films [34], because the films annealed in air form as particles of different sizes ordered in certain directions. This structure may be due to the effect of the surface and internal defects, which exist only during annealing in air, and act as nucleation centres to initiate crystal growth at about 673K [21]. Increasing dwell time the common decreased hardness in Fig. 3, at 473K, is in direction of equation 5. This is expected from the films being of amorphous state. The observed decrease of hardness with dwell time in, Fig. 4, as a common phenomenon [39] is indicative of the material undergoing creep deformation. About 673K, the amorphous films are partially transformed into the crystalline structure characterized by preferred orientation and growth on some crystallographic planes which have lower internal stresses, less orientation energy and small boundary angles. The start of crystallization is associated with increased hardness. At 873K, the complete crystallization is expected and the relief of internal stresses at a higher temperature is a factor contributing to the number of planes oriented in harmony to increase the intensity of a reflecting plane in the pattern. For Fig.4, on raising the temperature of TiO_2 thin film from room temperature, H_{Vf} decreased at 473K for all dwell times and showed independence on time, while H_{Vf} increased at 673K and then decreased at temperature 873K due to the growth of particles at this temperature.

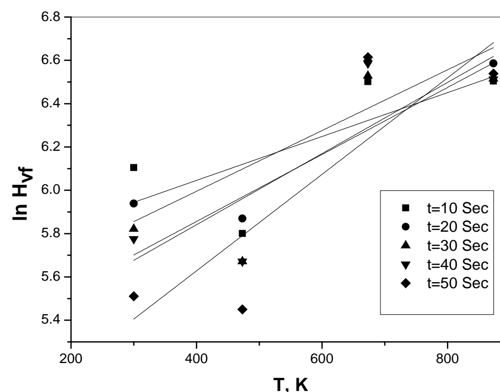

Fig.5: Plots of $\ln H_{vf}$ against temperature T for TiO_2 thin films annealed for different times.

From the straight lines given in Fig.5 and using equation 5, the softening coefficient, α,is obtained as the slope of the straight line and the intrinsic hardness H_0 is obtained from the intercept at $\ln H_{Vf}$ under different loads and dwell times for TiO_2 thin films.
The time dependence of, α, and H_0 are given in Fig.6 (a,b).

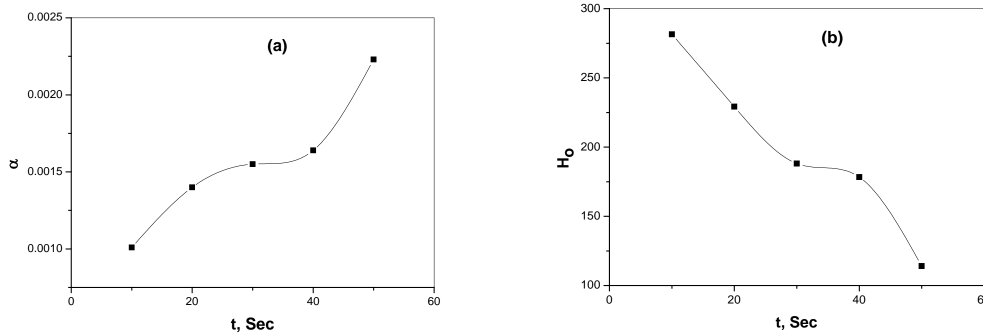

Fig.6: Time dependence of (a) α, and (b) Ho.

The log-log plot between 'p' and'd' of figure 7 yields almost a straight line graph. The slope determines the value of work hardening index 'n' at different dwell times. For the as deposited titanium dioxide film, from the graphs, 'n' values were found to be (1.58, 1.7, 1.77, 1.8 and 1.63) for the dwell times (10, 20, 30, 40, and 50 Sec) respectively. The lower the value of work hardening index, 'n', the better will be the hardness of the nano particle sized material [25].

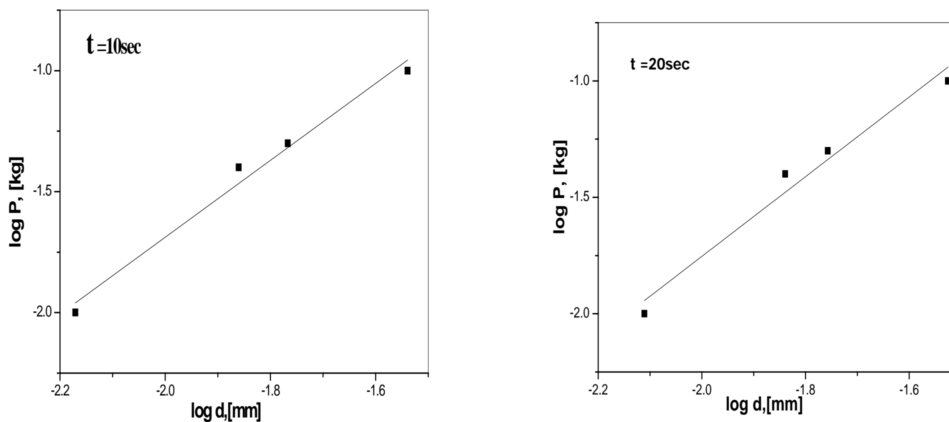

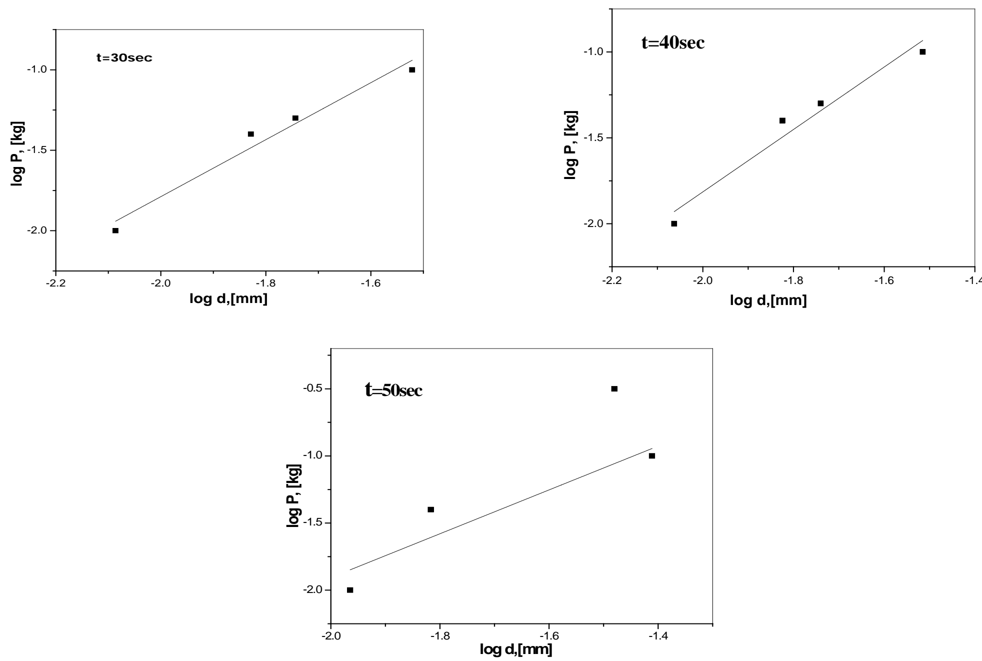

Fig.7: Plots log P vs. log d with different time (10, 20, 30, 40, and 50 sec) for TiO_2 thin film.

The work hardening index 'n' for the as deposited TiO_2 film was less than 2, showing that the hardness has a load dependent behaviour, i.e., Indentation- induced cracking phenomena and the apparent change in hardness value with change in indentation size, namely, the indentation size effect (ISE) [42]. This agrees well with previous investigations [43, 44].

In the discussion of the standard Vickers hardness test, the empirical expression of Meyer's law [45], which relates the applied load, p (in kg), and the impression diagonal, d (in mm), having the form:

$$p=ad^n \quad (6)$$

where, n, is the Meyer exponent, or (ISE), or the work hardening index, and, a, is the prefactor. This relation, when yields a constant value for the ISE index, n, of 2, then the hardness should be independent on indentation size. There is an increase in hardness at small loads for most metals and alloys, and therefore will be less than 2, showing that the hardness has a load dependent behaviour, i.e., ISE behaviour. This shows that the value of n suggests the presence of a weak ISE, as compared with the value 2 [45, 46].

Indentation creep experiments were carried out on TiO_2 films at the same temperature range, 300-873 K, using the loads 10, 50, 100 and 300 gm, as given in Fig.8.

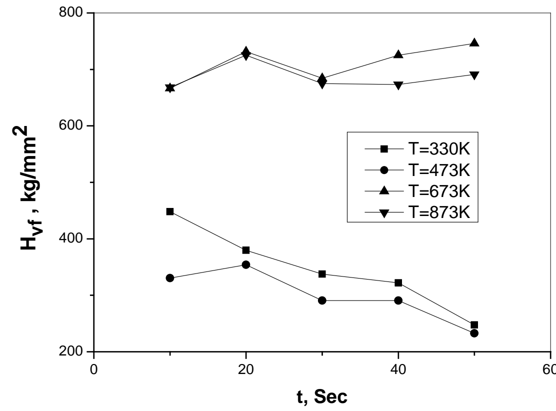

Figs.8: Plot of H_{vf} vs. time for TiO_2 thin film under different temperatures.

The log hardness versus log time data obtained from Fig.8, were plotted at different temperatures and given in Fig. 9. The equation derived by Sargent and Ashby [47] to analyze the obtained time dependent hardness data based on dimensional analysis is given as:

$$H(t) = (\sigma_o)/(mc\dot{\varepsilon}_o t)^{1/m} \quad (7)$$

where $H(t)$ is the time dependent hardness, $\dot{\varepsilon}_o$ is the strain rate at reference stress σ_o, c is a constant and m is the stress exponent.

IJSER

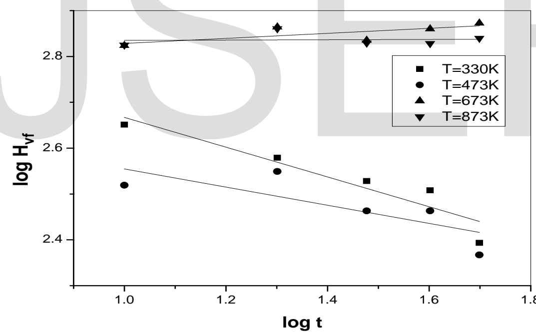

Figs.9: Relation between H_{vf} vs. time for TiO_2 thin film under different temperatures.

From the slope, in Fig. 9, the creep constant k is calculated and its negative inverse gives the stress exponent m. From the intercept with log H_{Vf} axis, the value of the hardness at reference time equals one second, H_1, is obtained. The time dependence of k, m and H_1 are given in Fig.10.

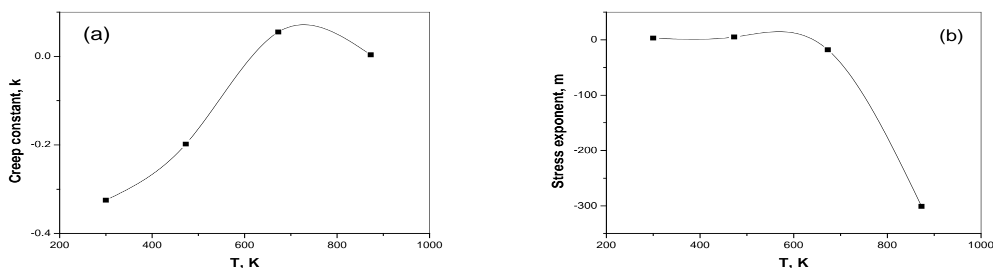

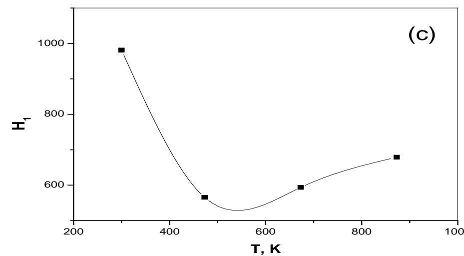

Figs.10: (a) creep constant, k, (b) stress exponent, m, (c) H_1.

Hardness measurements can be used in terms of mechanical parameters such as the relation between hardness H_{vf} and the yield stress σ_y, where [48]:

$$H_{vf} = 3\sigma_y \quad (8)$$

Applying equation (8), the temperature dependence of yield stress σ_y for TiO_2 thin films under different loads and dwell times, is given in Fig.11. The general behaviour of the curves of figs. 4 and 11 are the same, so that the parameters obtained from hardness can be easily obtained by using Eq. (8).

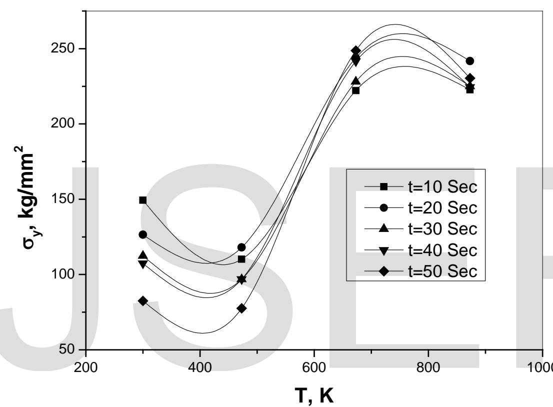

Fig.11: Temperature dependence of yield stress, σ_y, for the TiO_2 thin films as deduced from hardness data under different dwell times.

4. Conclusion

Thin films of Titanium dioxide were prepared by conventional thermal evaporation technique.

The XRD pattern of powder has a polycrystalline nature with average crystallite size, D, equals 30.266nm. It was found that annealing has an effect on XRD patterns of TiO_2 thin films.

SEM image of TiO_2 film prepared at room temperature, showed good uniformity, crack free surface and nanoparticles with small ellipsoidal shape dispersing in high separations. Annealed films at 473 – 873K showed the nature of amorphous film under tensile strain at 473K, and the change of TiO_2 anatase phase from amorphous-to-polycrystalline nature was observed after annealing at about 673K.

On increasing film thickness, the hardness decreased because of the decrease in film density. The absence of stable monotonic behaviour, for the, H_{Vf} -T, curves, on increasing temperature may be rendered to both the structural modifications responsible for changes in hardness levels, and the combined effects of the applied factors: temperature T, and dwell time t, under constant load on H_{Vf}.

Meyer index, n, for TiO_2 thin film was 1.6, so, there is size effect (ISE), and H_{Vf} depends on indentation size. The softening coefficient, α, increased and the intrinsic hardness, H_0, decreased on increasing time. Increasing the applied load, p, decreased and, H_0, increased.

References:

[1] H. Gleiter, Prog. *Mater. Sci*., 33(1989) 223-315.

[2] U. Diebold, *Surf. Sci. Rep.*, 48 (2003) 53-229.

[3] N .R. Mathews, M.A.C. Jacome, E.R. Morales, J. A.T. Antoniom, *Physica Status Solidi*, 6(2009) 219-223.

[4] A.M Gaur Member, IAENG, Rajat Joshi , Mukesh Kumar Member, *IAENG,Proceedings of the world congress on Engineering* 2011"Vol II WCE.

[5] T.Syganov, M. F. Maitz and E. Wieser, *Appl. Surf. Sci.*, 235 (2004) 156-163.

[6] L. Sikong, B. Kongreong, D. Kantachote, W. Sutthisripok, *Energy Research Journal, science publications*, (2010) 120-125.

[7] Q. Zhang, L. Gao and J. Guo.. *J. Eur. Ceram. Soc.*, 20(2000) 2153-2158.

[8] R. Paily, A. D. Gupta, N. D. Gupta, P. Bhattacharya, P. Misra, T. Ganguli, L. M. Kukreja, A. K. Balamurugan, S. Rajagopalan , A. K. Tyagi, *Appl. Surf. Sci.*, 187 (2002) 297.

[9] M. Landmann, E. Rauls and W. Schmidt, The electronic structure and opticalresponse of rutile, anatase and brookite TiO_2, *J. Phys*. 24(5) (2012) 1-6 .

[10] O. Carp, C.L. Huisman, A. Reller, *Progress in Solid State Chemistry* 32 (2004) 33–177.

[11] L. Kavan, D. Fattakhova, P. Krtil, *J Electrochem Soc*, 146 (1999) 375.

[12] R. Vijayalakshmi and V. Rajendran.,*Arch. Appl. Sci. Res*., 4 (2)(2012) 1183-1190.

[13] A. M. Ali, and S. R. Sani, *Journal Of Nanostructure in Chemistry*, 3 (2013) 35.

[14] S.Tolansky, Multiple-Beam Interference Microscopy of Metals, *Academic Press, London* (1970) p.55.

[15] H. Buckle, Metal Rev., 4 (1959) 49.

[16] I.V. Osttovskii, A. Nadtochii, Phys. of the Solid State, 42 (2000) 8.

[17] C.S. Roberts, in: Magnesium and its alloys, John Willey and Sons, New York (1960) p. 26.

[18] W.A. Spitzing, and P.D. Krotz, Acta Metall. 36, 1709 (1988).

[19] A. M Korsunsky, M.R McGurk, S.J Bull and T. F Page; *Surf. Coat. Technoal*. 99 (1998) 171.

[20] VD Mote, Y Purushotham, and BN Dole, Journal of Theoretical and Applied Physics (2012) 6:6.

[21] T. A. Witten, L. M. Sander, *Phys. ReV. Lett.,* 47 (19)(1981)1400- 1403.

[22] N.R. Mathews, Erik R. Morales, M.A. Corte´s-Jacome, J.A. Toledo Antonio, *Solar Energy* 83 (2009) 1499–1508.

[23] F. Abd El-Salam, R.H.Nada, H. Abd El Aziz, E. Abd El-Rheim, *Egypt. J. Solids*, 33(2) (2010) 265- 280.

[24] G. Sharma, R. V. Ramanujan, T. R. G. Kutty , G. P. Tiwari ,*Mater. Sci. Eng. A* 278 (2000) 106.

[25] U. Ullas Pradhan , S. K. Naveen Kumar, *Archives of Physics Research*,2 (4)(2011) 121-127.

[26] I. Manika and J.Maniks; *J. Phys. D: Appl. Phys*. 41 (2008) 074010.

[27] P. J. BURNETT AND D. S. RICKERBY, *Thin Solid Films*, 154 (1987) 403-416 403.

IJSER

[28] H. Buckle, in J. W. Westbrook and H. Conrad (eds.), *Science of Hardness Testing und its Researc Applications,* American Society for Metals, Metals Park, OH. p. 453.
[29] B. Jonsson and S. Hogmark, *Thin Solid Films, 1 I4 (1984) 257-269.*
[30] P. J. Burnett and D. S. Rickerby, *Thin SolidFilms, 40 (148) (1987)* 51.
[31] J.L He, W.Z Li, and H.D Li, *Appl. Phys. Letters* 69 (1996) 1402.
[32] J.L He and S Veprek , *Surf. Coat. Technoal* 374 (2003)163-164.
[33] A. James Corno, S. John, Y. Rusen, and L. G. James,*J. Phys. Chem. C*, 112 (14)(2008)5439-5446.
[34] F. Abd El-Salam, M. A. Afify, and E. Abd El- Wahabb, *Vacuum* 44(10) (1993)1009- 1013.
[35] F. Abd El-Salam and E. Abd El- Wahabb, *Vacuum* , 43(1992) 849- 853.
[36] F. Abd El-Salam, A. M. Abd El- Khalek, R.H.Nada, A. Fawzy; *Materials Characterization*, 59(2008) 9- 17.
[37] H.Tang, F.Levy, H Berger, P.E. Schmid,. *Physical Review*, 52 (11) (1995) 7771–7774.
[38] K. Balachandaran, R.Venckatesh, Rajeshwari Sivaraj, *IJEST* 3 (5) (2011) .
[39] F. Abd El-salam, L. A. Wahab, R. H. Nada and H. Y. Zahran; *J. Mater. Sci*. (42) (2007) 3661-3669.
[40] F.J. Batla Calleja Flores, A. Ania F. and D.C. Basset; *J.Mater.Sci*. (35) (2000) 1315- 1319.
[41] F. J. Batla Calleja; *Trends Polym. Sci*. (66) (1985) 17.
[42] X. Cal, X. Yang and P. Zhou; J. *Mater. Sci. Lett*. 16 (1997) 741-742.
[43] Yu-Lan Lin, Ting-Jie Wang), Yong Jin, *Elsevier, Powder Technology* 123(2002) 194–198.
[44] H. Li, R.C. bradt, J.Mater.Sci. 28 (1993) 917-926.
[45] I. Manika and J.Manika; *Acta Materialia* 54 (2006) 2049 .
[46] C. J. Wang, C. Y. Huang, *Materials Science and Engineering A* 492 (2008) 306–310.
[47] P. M. Sargent, M. F. Ashby, *Mater. Sci. Tech.* 8 (1992) 594.
[48] E. R. Petty, H. Ốneill, *Metallurgia*, (63) (1961) 25.

IJSER